CHAPTER 29
STRENGTH UNDER DYNAMIC CONDITIONS

Charles R. Mischke, Ph.D., P.E.
Professor Emeritus of Mechanical Engineering
Iowa State University
Ames, Iowa

29.1 TESTING METHODS AND PRESENTATION OF RESULTS / 29.3
29.2 SN DIAGRAM FOR SINUSOIDAL AND RANDOM LOADING / 29.7
29.3 FATIGUE-STRENGTH MODIFICATION FACTORS / 29.9
29.4 FLUCTUATING STRESS / 29.18
29.5 COMPLICATED STRESS-VARIATION PATTERNS / 29.20
29.6 STRENGTH AT CRITICAL LOCATIONS / 29.22
29.7 COMBINED LOADING / 29.27
29.8 SURFACE FATIGUE / 29.32
REFERENCES / 29.35
RECOMMENDED READING / 29.36

NOMENCLATURE

a	Distance, exponent, constant
A	Area, addition factor, ΣiN_i
b	Distance, width, exponent
B	$\Sigma i^2 N_i$
bhn	Brinell hardness, roller or pinion
BHN	Brinell hardness, cam or gear
c	Exponent
C	Coefficient of variation
C_p	Materials constant in rolling contact
d	Difference in stress level, diameter
d_e	Equivalent diameter
D	Damage per cycle or block of cycles
D_I	Ideal critical diameter
E	Young's modulus
f	Fraction of mean ultimate tensile strength
f_i	Fraction of life measure

F	Force
$\mathscr{F}$	Significant force in contact fatigue
h	Depth
H_B	Brinell hardness
I	Second area moment
k_a	Marin surface condition modification factor
k_b	Marin size modification factor
k_c	Marin load modification factor
k_d	Marin temperature modification factor
k_e	Marin miscellaneous-effects modification factor
K	Load-life constant
K_f	Fatigue stress concentration factor
K_t	Geometric (theoretical) stress concentration factor
ℓ	Length
log	Base 10 logarithm
ln	Natural logarithm
L	Life measure
LN	Lognormal
m	Strain-strengthening exponent, revolutions ratio
M	Bending moment
$\mathbf{n}, n$	Design factor
N	Cycles
N_f	Cycles to failure
$N(\mu, \sigma)$	Normal distribution with mean μ and standard deviation σ
p	Pressure
P	Axial load
q	Notch sensitivity
r	Notch radius, slope of load line
r_i	Average peak-to-valley distance
R	Reliability
R_a	Average deviation from the mean
R_{rms}	Root-mean-squared deviation from the mean
RA	Fraction reduction in area
R_Q	As-quenched hardness, Rockwell C scale
R_T	Tempered hardness, Rockwell C scale
S	Strength
S'_{ax}	Axial endurance limit
S'_e	Rotating-beam endurance limit
S_f	Fatigue strength

S'_{se}	Torsional endurance limit
S_u, S_{ut}	Ultimate tensile strength
S_y	Yield strength
t_f	Temperature, °F
T	Torque
w	Width
x	Variable, coordinate
y	Variable, coordinate
z	Variable, coordinate, variable of $N(0, z)$
α	Prot loading rate, psi/cycle
β	Rectangular beam width
Δ	Approach of center of roller
ε	True strain
ε_f	True strain at fracture
η	Factor of safety
θ	Angle, misalignment angle
λ	Lognormally distributed
μ	Mean
ν	Poisson's ratio
ξ	Normally distributed
σ	Normal stress
σ_a	Normal stress amplitude component
σ'_f	Fatigue strength coefficient
σ_m	Steady normal stress component
$\sigma_{\max}$	Largest normal stress
$\sigma_{\min}$	Smallest normal stress
σ_0	Nominal normal stress
$\overline{\sigma}_0$	Strain-strengthening coefficient
σ	Standard deviation
τ	Shear stress
ϕ	Pressure angle

29.1 TESTING METHODS AND PRESENTATION OF RESULTS

The designer has need of knowledge concerning endurance limit (if one exists) and endurance strengths for materials specified or contemplated. These can be estimated from the following:

- Tabulated material properties (experience of others)
- Personal or corporate R. R. Moore endurance testing
- Uniaxial tension testing and various correlations
- For plain carbon steels, if heat treating is involved, Jominy test and estimation of tempering effects by the method of Crafts and Lamont
- For low-alloy steels, if heat treating is involved, prediction of the Jominy curve by the method of Grossmann and Fields and estimation of tempering effects by the method of Crafts and Lamont
- If less than infinite life is required, estimation from correlations
- If cold work or plastic strain is an integral part of the manufacturing process, using the method of Datsko

The representation of data gathered in support of fatigue-strength estimation is best made probabilistically, since inferences are being made from the testing of necessarily small samples. There is a long history of presentation of these quantities as deterministic, which necessitated generous design factors. The plotting of cycles to failure as abscissa and corresponding stress level as ordinate is the common SN curve. When the presentation is made on logarithmic scales, some piecewise rectification may be present, which forms the basis of useful curve fits. Some ferrous materials exhibit a pronounced knee in the curve and then very little dependency of strength with life. Deterministic researchers declared the existence of a zero-slope portion of the curve and coined the name *endurance limit* for this apparent asymptote.

Based on many tests over the years, the general form of a steel SN curve is taken to be approximately linear on log-log coordinates in the range 10^3 to 10^6 cycles and nearly invariant beyond 10^7 cycles. With these useful *approximations* and knowledge that cycles-to-failure distributions at constant stress level are lognormal and that stress-to-failure distributions at constant life are likewise lognormal, specialized methods can be used to find some needed attribute of the SN picture. The cost and time penalties associated with developing the complete picture motivate the experimentor to seek only what is needed.

29.1.1 Sparse Survey

On the order of a dozen specimens are run to failure in an R. R. Moore apparatus at stress levels giving lives of about 10^3 to 10^7 cycles. The points are plotted on log-log paper, and in the interval $10^3 < N < 10^7$ cycles, a "best" straight line is drawn. Those specimens which have not failed by 10^8 or 5×10^8 cycles are used as evidence of the existence of an endurance limit. All that this method produces is estimates of two median lines, one of the form

$$S'_f = CN^b \qquad 10^3 < N < 10^6 \tag{29.1}$$

and the other of the form

$$S'_f = S'_e \qquad N > 10^6 \tag{29.2}$$

This procedure "roughs in" the SN curve as a gross estimate. No standard deviation information is generated, and so no reliability contours may be created.

29.1.2 Constant-Stress-Level Testing

If high-cycle fatigue strength in the range of 10^3 to 10^6 cycles is required and reliability (probability of survival) contours are required, then constant-stress-level testing is useful. A dozen or more specimens are tested at each of several stress levels. These results are plotted on lognormal probability paper to "confirm" by inspection the lognormal distribution, or a statistical goodness-of-fit test (Smirnov-Kolomogorov, chi-squared) is conducted to see if lognormal distribution can be rejected. If not, then reliability contours are established using lognormal statistics. Nothing is learned about endurance limit. Sixty to 100 specimens usually have been expended.

29.1.3 Probit Method

If statistical information (mean, standard deviation, distribution) concerning the endurance limit is needed, the probit method is useful. Given a priori knowledge that a "knee" exists, stress levels are selected that at the highest level produce one or two runouts and at the lowest level produce one or two failures. This places the testing at the "knee" of the curve and within a couple of standard deviations on either side of the endurance limit. The method requires exploratory testing to estimate the stress levels that will accomplish this. The results of the testing are interpreted as a lognormal distribution of stress either by plotting on probability paper or by using a goodness-of-fit statistical reduction to "confirm" the distribution. If it is confirmed, the mean endurance limit, its variance, and reliability contours can be expressed. The existence of an endurance limit has been assumed, not proven. With specimens declared runouts if they survive to 10^7 cycles, one can be fooled by the "knee" of a nonferrous material which exhibits no endurance limit.

29.1.4 Coaxing

It is intuitively appealing to think that more information is given by a failed specimen than by a censored specimen. In the preceding methods, many of the specimens were unfailed (commonly called *runouts*). Postulating the existence of an endurance limit and no damage occurring for cycles endured at stress levels less than the endurance limit, a method exists that raises the stress level of unfailed (by, say, 10^7 cycles) specimens to the next higher stress level and tests to failure starting the cycle count again. Since every specimen fails, the specimen set is smaller. The results are interpreted as a normal stress distribution. The method's assumption that a runout specimen is neither damaged nor strengthened complicates the results, since there is evidence that the endurance limit can be enhanced by such coaxing [29.1].

29.1.5 Prot Method†

This method involves steadily increasing the stress level with every cycle. Its advantage is reduction in number of specimens; its disadvantage is the introduction of (1) coaxing, (2) an empirical equation, that is,

$$S_\alpha = S'_e + K\alpha^n \tag{29.3}$$

† See Ref. [29.2].

where S_α = Prot failure stress at loading rate, α psi/cycle
S_e' = material endurance limit
K, n = material constants
α = loading rate, psi/cycle

and (3) an extrapolation procedure. More detail is available in Collins [29.3].

29.1.6 Up-Down Method†

The up-down method of testing is a common scheme for reducing R. R. Moore data to an estimate of the endurance limit. It is adaptable to seeking endurance strength at any arbitrary number of cycles. Figure 29.1 shows the data from 54 specimens

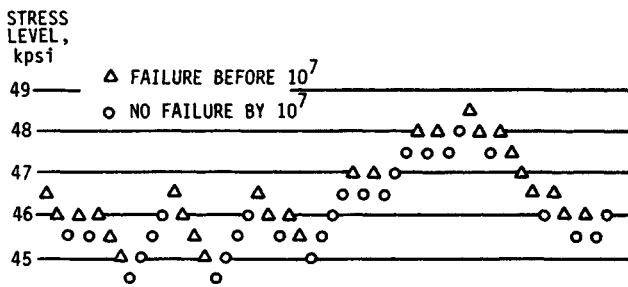

FIGURE 29.1 An up-down fatigue test conducted on 54 specimens. *(From Ransom [29.5], with permission.)*

gathered for determining the endurance strength at 10^7 cycles. The step size was 0.5 kpsi. The first specimen at a stress level of 46.5 kpsi failed before reaching 10^7 cycles, and so the next lower stress level of 46.0 kpsi was used on the subsequent specimen. It also failed before 10^7 cycles. The third specimen, at 45.5 kpsi, survived 10^7 cycles, and so the stress level was increased. The data-reduction procedure eliminates specimens until the first runout-fail pair is encountered. We eliminate the first specimen and add as an observation the next (no. 55) specimen, $\sigma = 46.5$ kpsi. The second step is to identify the least frequent event—failures or runouts. Since there are 27 failures and 27 runouts, we arbitrarily choose failures and tabulate N_i, iN_i, and i^2N_i as shown in Table 29.1. We define $A = \Sigma iN_i$ and $B = \Sigma i^2N_i$. The estimate of the mean of the 10^7-cycle strength is

$$\hat{\mu} = S_0 + d\left(\frac{A}{\Sigma N_i} \pm \frac{1}{2}\right) \tag{29.4}$$

where S_0 = the lowest stress level on which the less frequent event occurs, d = the stress-level increment or step, and N_i = the number of less frequent events at stress level σ_i. Use +½ if the less frequent event is runout and −½ if it is failure. The estimate of the mean 10^7-cycle strength is

† See Refs. [29.4] and [29.5].

TABLE 29.1 Extension of Up-Down Fatigue Data

Stress level, kpsi	Coded level	Class failures		
		N_i	iN_i	i^2N_i
48.5	7	1	7	49
48.0	6	4	24	144
47.5	5	1	5	25
47.0	4	3	12	48
46.5	3	5	15	45
46.0	2	8	16	32
45.5	1	3	3	3
45.0	0	2	0	0
		Σ 27	82	346

$$\hat{\mu} = 45.0 + 0.5\left(\frac{82}{27} - \frac{1}{2}\right) = 46.27 \text{ kpsi}$$

The standard deviation is

$$\hat{\sigma} = 1.620d\left[\frac{B\Sigma N_i - A^2}{(\Sigma N_i)^2} + 0.029\right] \tag{29.5}$$

as long as $(B\Sigma N_i - A^2)/(\Sigma N_i)^2 \geq 0.3$. Substituting test data into Eq. (29.5) gives

$$\hat{\sigma} = 1.620(0.5)\left[\frac{342(27) - 82^2}{27^2} + 0.029\right] = 2.93 \text{ kpsi}$$

The result of the up-down test can be expressed as $(S_f')_{10^7}(\hat{\mu}, \hat{\sigma})$ or $(S_f')_{10^7}(46.27, 2.93)$. Consult Refs. [29.3] and [29.4] for modification of the usual t-statistic method of placing a confidence interval on μ and Ref. [29.4] for placing a confidence interval on σ. A point estimate of the coefficient of variation is $\sigma/\mu = 2.93/46.27$, or 0.063. Coefficients of variation larger than 0.1 have been observed in steels. One must examine the sources of tables that display a single value for an endurance strength to discover whether the mean or the smallest value in a sample is being reported. This can also reveal the coefficient of variation.

29.2 SN DIAGRAM FOR SINUSOIDAL AND RANDOM LOADING

The usual presentation of R. R. Moore testing results is on a plot of S_f' (or S_f'/S_u) versus N, commonly on log-log coordinates because segments of the locus appear to be rectified. Figure 29.2 is a common example. Because of the dispersion in results, sometimes a $\pm 3\sigma$ band is placed about the median locus or (preferably) the data points are shown as in Fig. 29.3. In any presentation of this sort, the only things that might be true are the observations. All lines or loci are curve fits of convenience, there being no theory to suggest a rational form. What will endure are the data and

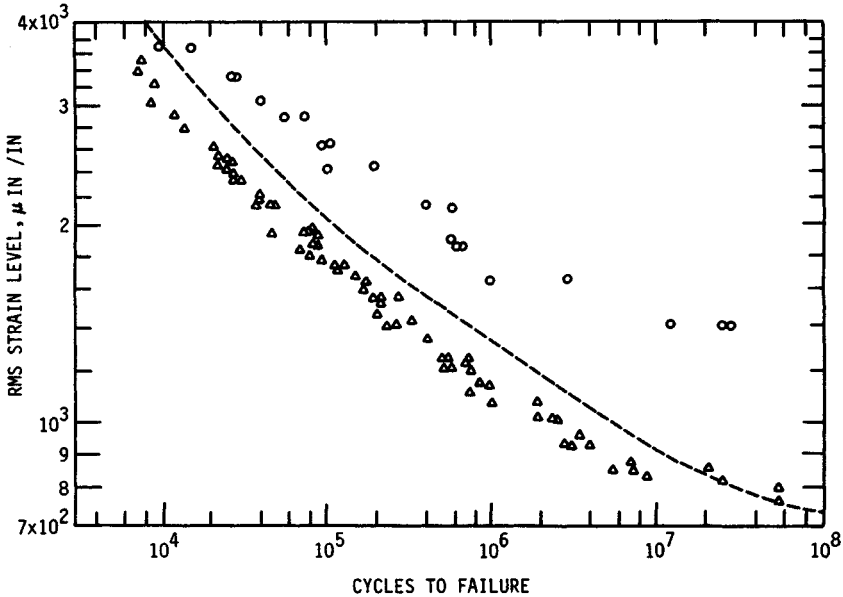

FIGURE 29.2 Fatigue data on 2024-T3 aluminum alloy for narrow-band random loading, △, and for constant-amplitude loading, ○. *(Adapted with permission from Haugen [29.14], p. 339.)*

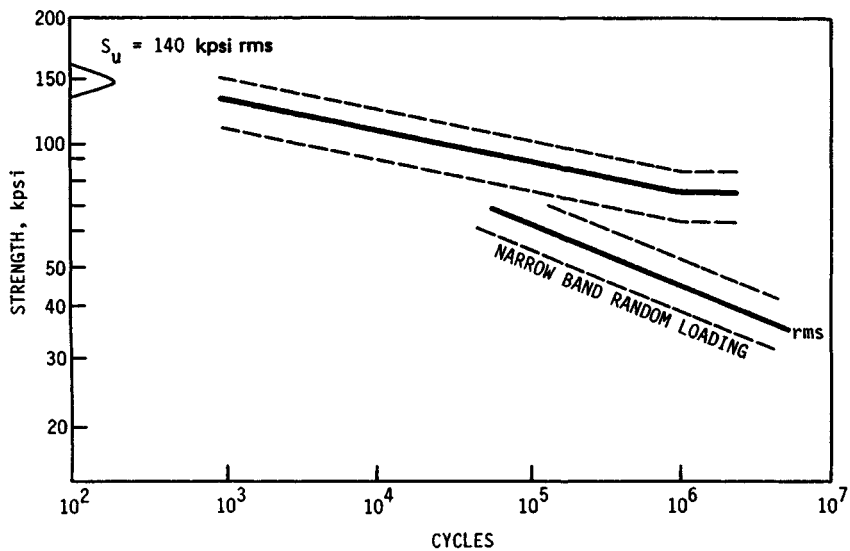

FIGURE 29.3 Statistical SN diagram for constant-amplitude and narrow-band random loading for a low-alloy steel. Note the absence of a "knee" in the random loading.

not the loci. Unfortunately, too much reported work is presented without data; hence early effort is largely lost as we learn more.

The R. R. Moore test is a sinusoidal completely reversed flexural loading, which is typical of much rotating machinery, but not of other forms of fatigue. Narrow-band random loading (zero mean) exhibits a lower strength than constant-amplitude sine-wave loading. Figure 29.3 is an example of a distributional presentation, and Fig. 29.2 shows the difference between sinusoidal and random-loading strength.

29.3 FATIGUE-STRENGTH MODIFICATION FACTORS

The results of endurance testing are often made available to the designer in a concise form by metals suppliers and company materials sections. Plotting coordinates are chosen so that it is just as easy to enter the plot with maximum-stress, minimum-stress information as steady and alternating stresses. The failure contours are indexed from about 10^3 cycles up to about 10^9 cycles. Figures 29.4, 29.5, and 29.6 are

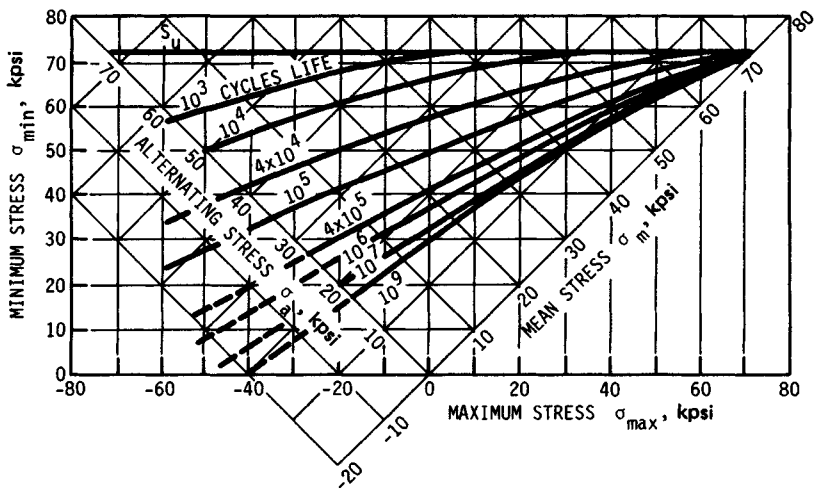

FIGURE 29.4 Fatigue-strength diagram for 2024-T3, 2024-T4, and 2014-T6 aluminum alloys, axial loading. Average of test data for polished specimens (unclad) from rolled and drawn sheet and bar. Static properties for 2024: $S_u = 72$ kpsi, $S_y = 52$ kpsi; for 2014: $S_u = 72$ kpsi, $S_y = 63$ kpsi. *(Grumman Aerospace Corp.)*

examples. The usual testing basis is bending fatigue, zero mean, constant amplitude. Figure 29.6 represents axial fatigue. The problem for the designer is how to adjust this information to account for all the discrepancies between the R. R. Moore specimen and the contemplated machine part. The Marin approach [29.6] is to introduce multiplicative modification factors to adjust the endurance limit, in the deterministic form

$$S_e = k_a k_b k_c k_d k_e S'_e \tag{29.6}$$

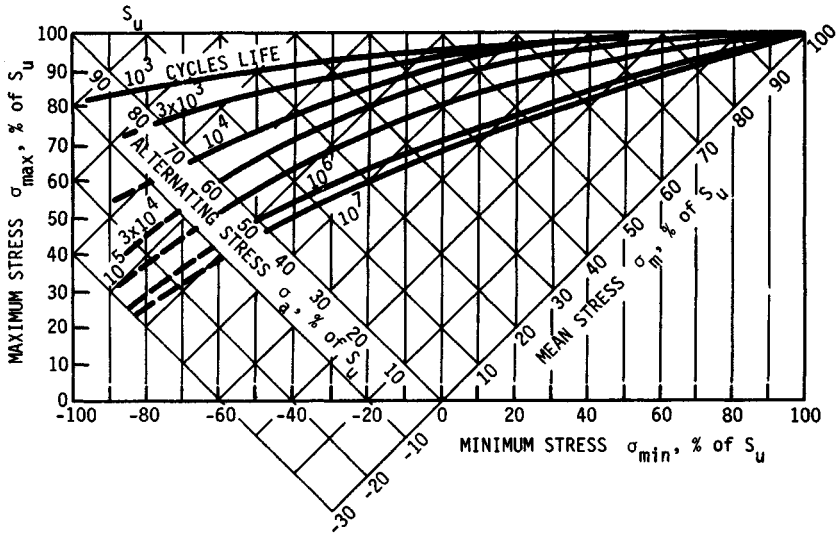

FIGURE 29.5 Fatigue-strength diagram for alloy steel, S_u = 125 to 180 kpsi, axial loading. Average of test data for polished specimens of AISI 4340 steel (also applicable to other alloy steels, such as AISI 2330, 4130, 8630). *(Grumman Aerospace Corp.)*

FIGURE 29.6 Fatigue-strength diagram for 7075-T6 aluminum alloy, axial loading. Average of test data for polished specimens (unclad) from rolled and drawn sheet and bar. Static properties: S_u = 82 kpsi, S_y = 75 kpsi. *(Grumman Aerospace Corp.)*

where k_a = surface condition modification factor
k_b = size modification factor
k_c = loading modification factor
k_d = temperature modification factor
k_e = miscellaneous-effects modification factor
S'_e = endurance limit of rotating-beam specimen
S_e = endurance limit at critical location of part in the geometry and condition of use

29.3.1 Marin Surface Factor k_a

The Marin surface condition modification factor for steels may be expressed in the form

$$k_a = aS_{ut}^b \tag{29.7}$$

Table 29.2 gives values of a, b for various surface conditions. See also Fig. 29.7.

TABLE 29.2 Parameters of Marin Surface Condition Factor

	a		
Surface finish	kpsi	MPa	b
Ground	1.34	1.58	–0.086
Machined, cold-rolled	2.67	4.45	–0.265
Hot-rolled	14.5	58.1	–0.719
As-forged	39.8	271	–0.995

Source: Data from C. G. Noll and C. Lipson, "Allowable Working Stresses," *Society of Experimental Stress Analysis,* vol. 3, no. 2, 1946, p. 49, reduced from their graphed data points.

Example 1. A steel has a mean ultimate tensile strength of 520 MPa and a machined surface. Estimate k_a.

Solution: From Table 29.2,

$$k_a = 4.45(520)^{-0.265} = 0.848$$

29.3.2 Marin Size Factor k_b

In bending and torsion, where a stress gradient exists, Kuguel observed that the volume of material stressed to 0.95 or more of the maximum stress controls the risk of encountering a crack nucleation, or growth of an existing flaw becoming critical. The equivalent diameter d_e of the R. R. Moore specimen with the same failure risk is

$$d_e = \sqrt{\frac{A_{0.95}}{0.076\,576}} \tag{29.8}$$

where $A_{0.95}$ is the cross-sectional area exposed to 95 percent or more of the maximum stress. For a round in rotating bending or torsion, $A_{0.95} = 0.075\,575d^2$. For a round in nonrotating bending, $A_{0.95} = 0.010\,462d^2$. For a rectangular section $b \times h$ in

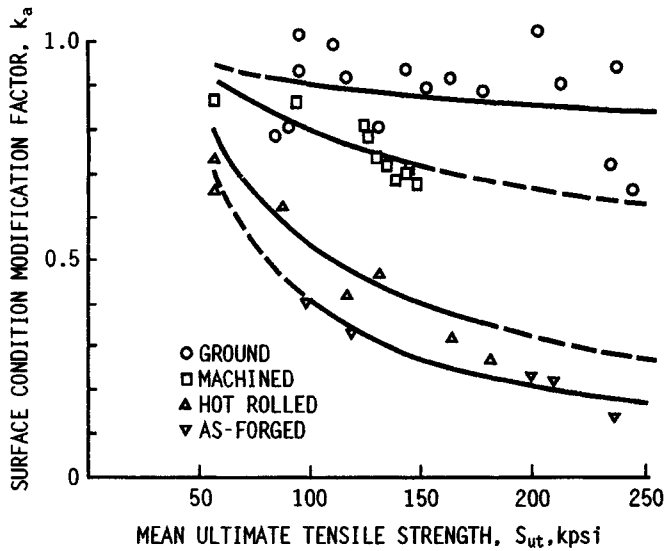

FIGURE 29.7 Marin endurance limit fatigue modification factor k_a for various surface conditions of steels. See also Table 29.2.

bending, $A_{0.95} = 0.05bh$. See [29.6], p. 284 for channels and I-beams in bending. Table 29.3 gives useful relations. In bending and torsion,

$$k_b = \begin{cases} (d_e/0.30)^{-0.107} = 0.879d_e^{-0.107} & d_e \text{ in inches} \quad (29.9) \\ (d_e/7.62)^{-0.107} = 1.24d_e^{-0.107} & d_e \text{ in mm} \quad (29.10) \end{cases}$$

For axial loading, $k_b = 1$. Table 29.4 gives various expressions for k_b. The Marin size factor is scalar (deterministic). At less than standard specimen diameter (0.30 in), many engineers set $k_b = 1$.

29.3.3 Marin Loading Factor k_c

The Marin loading factor k_c can be expressed as

$$k_c = \alpha S_{ut}^{\beta} \quad (29.11)$$

TABLE 29.3 Equivalent Diameters for Marin Size Factor

Section	Equivalent diameter d_e
Round, rotary bending, torsion	d
Round, nonrotating bending	$0.37d$
Rectangle, nonrotating bending	$0.808bh$

TABLE 29.4 Quantitative Expression for Size Factor

Expression	Range	Proposer
$k_b = \dfrac{0.947}{1 - 0.016/d}$	$0.125 \le d \le 1.875$ in	Moore
$k_b = 0.931\left(1 + \dfrac{0.014}{0.1 + d^2}\right)$	$d \ge 2$ in	Heywood
$k_b = \begin{cases} 0.869d^{-0.097} \\ 1 \\ 1.189d^{-0.97} \end{cases}$	$0.3 < d < 10$ in $d \le 0.3$ in or $d \le 8$ mm $8 < d \le 250$ mm	Shigley and Mitchell
$k_b = \begin{cases} 1 \\ 0.9 \\ 0.8 \\ 0.7 \end{cases}$	$d < 0.4$ in or 10 mm (0.4 in or 10 mm) $< d <$ (2 in or 50 mm) (2 in or 50 mm) $< d <$ (4 in or 100 mm) (4 in or 100 mm) $< d <$ (5 in or 150 mm)	Juvinall
$k_b = 1 - \dfrac{d - 0.3}{15}$	$2 \le d \le 9$ in	Roark

Table 29.5 gives values for α, β. For axial loading of steel based on Table 29.5, Table 29.6 was prepared. Juvinall [29.12] reports that for steel, $0.75 < \bar{k}_c < 1.0$, and suggests using $k_c = 0.90$ for accurate control of loading eccentricity and $0.60 < k_c < 0.85$ otherwise. The problem of load eccentricity plagues testing as well as the designer. Axial loading in fatigue requires caution. See Fig. 29.8.

For torsion, Table 29.7 summarizes experimental experience. In metals described by distortion-energy failure theory, the average value of k_c would be 0.577.

29.3.4 Marin Temperature Factor k_d

Steels exhibit an increase in endurance limit when temperatures depart from ambient. For temperatures up to about 600°F, such an increase is often seen, but above 600°F, rapid deterioration occurs. See Fig. 29.9. If specific material endurance limit–temperature testing is not available, then an ensemble of 21 carbon and alloy

TABLE 29.5 Parameters of Marin Loading Factor

	α		
Mode of loading	kpsi	MPa	β
Bending	1	1	0
Axial	1.23	1.43	−0.078
Torsion	0.328	0.258	0.125

TABLE 29.6 Marin Loading Factor for Axial Loading

S_{ut}, kpsi	$\bar{k}_c$†
50	0.907
100	0.859
150	0.822
200	0.814

† Average entry is 0.853.

TABLE 29.7 Torsional Loading, k_c

Material	Range k_c	$(k_c)_{avg}$
Wrought steels	0.52–0.69	0.60
Wrought Al	0.43–0.74	0.55
Wrought Cu and alloys	0.41–0.67	0.56
Wrought Mg and alloys	0.49–0.61	0.54
Titaniums	0.37–0.57	0.48
Cast irons	0.79–1.01	0.90
Cast Al, Mg, and alloys	0.71–0.91	0.85

steels gives, for t_f in °F,

$$k_d = [0.975 + (0.432 \times 10^{-3})t_f - (0.115 \times 10^{-5})t_f^2 + (0.104 \times 10^{-8})t_f^3 - (0.595 \times 10^{-12})t_f^4]$$

$$70 < t_f < 600°\text{F} \tag{29.12}$$

which equation may be useful. The distribution of k_d is lognormal. See Fig. 29.9 for some specific materials.

29.3.5 Stress Concentration and Notch Sensitivity

The modified Neuber equation (after Heywood) is

$$K_f = \frac{K_t}{1 + \dfrac{2}{\sqrt{r}} \dfrac{K_t - 1}{K_t} \sqrt{a}} \tag{29.13}$$

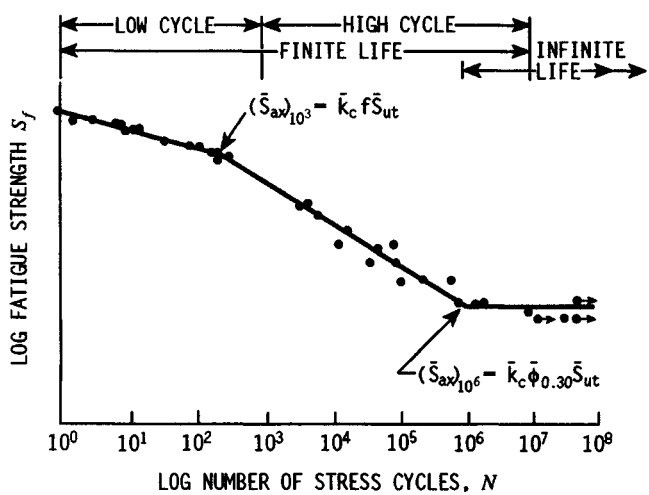

FIGURE 29.8 An SN diagram plotted from the results of completely reversed axial fatigue tests on a normalized 4130 steel, S_{ut} = 116 kpsi (data from NACA *Tech. Note* 3866, Dec. 1966).

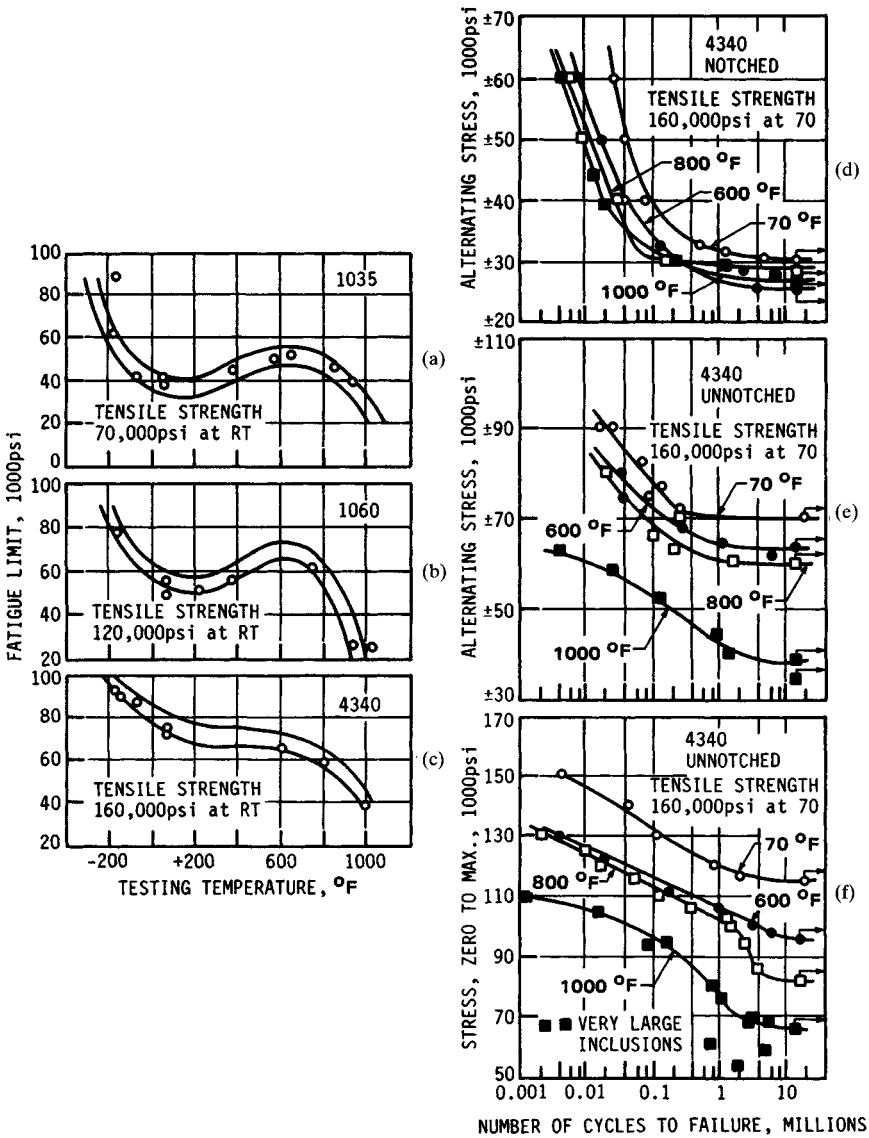

FIGURE 29.9 Effect of temperature on the fatigue limits of three steels: (*a*) 1035; (*b*) 1060; (*c*) 4340; (*d*) 4340, completely reversed loading $K = 3$ to 3.5; (*e*) 4340, completely reversed loading, unnotched; (*f*) 4340, repeatedly applied tension. *(American Society for Metals.)*

Table 29.8 gives values of $\sqrt{a}$. The stress-concentration factor K_f may be applied to the nominal stress σ_0 as $K_f\sigma_0$ as an augmentation of stress (preferred) or as a strength reduction factor $k_e = 1/K_f$ (sometimes convenient).

The finite life stress-concentration factor for steel for N cycles is obtained from the notch sensitivities $(q)_{10^3}$ and $(q)_{10^6}$. For 10^3 cycles,

TABLE 29.8 Heywood's Parameters, Eq. (29.13), Stress Concentration

Feature	$\sqrt{a}$ Using $\bar{S}_{ut}$, kpsi	$\sqrt{a}$ Using $\bar{S}'_e$, kpsi	$\sqrt{a}$ Using $\bar{S}_{ut}$, MPa	$\sqrt{a}$ Using $\bar{S}'_e$, MPa
Transverse hole	$5/S_{ut}$	$2.5/S'_e$	$174/S_{ut}$	$87/S'_e$
Shoulder	$4/S_{ut}$	$2/S'_e$	$139/S_{ut}$	$69.5/S'_e$
Groove	$3/S_{ut}$	$1.5/S'_e$	$104/S_{ut}$	$52/S'_e$

$$(q)_{10^3} = \frac{(K_f)_{10^3} - 1}{K_t - 1}$$

$$= -0.18 + (0.43 \times 10^{-2})\bar{S}_{ut} - (0.45 \times 10^{-5})\bar{S}_{ut}^2 \tag{29.14}$$

where $\bar{S}_{ut} < 330$ kpsi. For 10^6 cycles,

$$(q)_{10^6} = \frac{(K_f)_{10^6} - 1}{K_t - 1} \tag{29.15}$$

and for N cycles,

$$(K_f)_N = (K_f)_{10^3}\left[\frac{(K_f)_{10^6}}{(K_f)_{10^3}}\right]^{(1/3 \log N - 1)} \tag{29.16}$$

There is some evidence that $\overline{K}_f$ does not exceed 4 for Q&T steels and 3 for annealed steels [29.11]. Figure 29.10 shows scatter bands, and Fig. 29.11 relates notch radius to notch sensitivity.

29.3.6 Miscellaneous-Effects Modification Factor k_e

There are other effects in addition to surface texture, size loading, and temperature that influence fatigue strength. These other effects are grouped together because their influences are not always present, and are not well understood quantitatively in any comprehensive way. They are largely detrimental ($\bar{k}_e < 1$), and consequently cannot be ignored. For each effect present, the designer must make an estimate of the magnitude and probable uncertainty of k_e. Such effects include

- Introduction of complete stress fields due to press or shrink fits, hydraulic pressure, and the like
- Unintentional residual stresses that result from grinding or heat treatment and intentional residual stresses that result from shot peening or rolling of fillets
- Unintended coatings, usually corrosion products, and intentional coatings, such as plating, paint, and chemical sheaths
- Case hardening for wear resistance by processes such as carburization, nitriding, tuftriding, and flame and induction hardening
- Decarburizing of surface material during processing

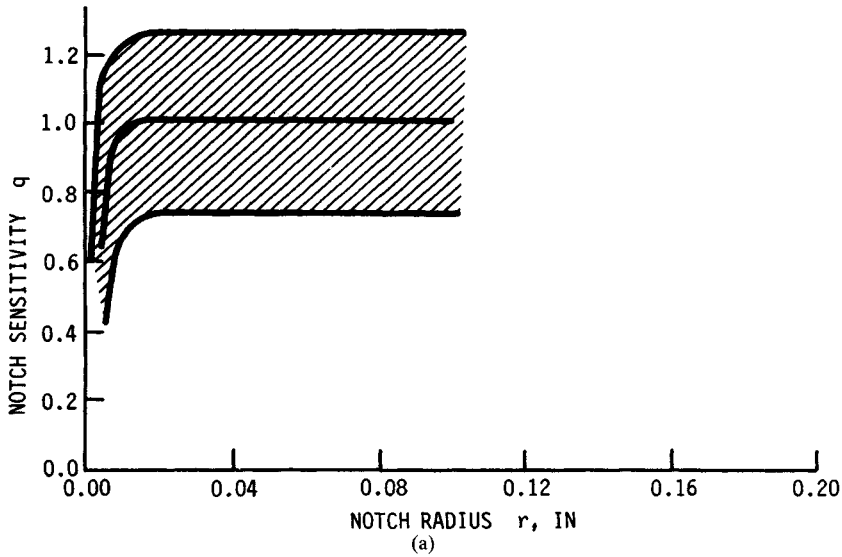

(a)

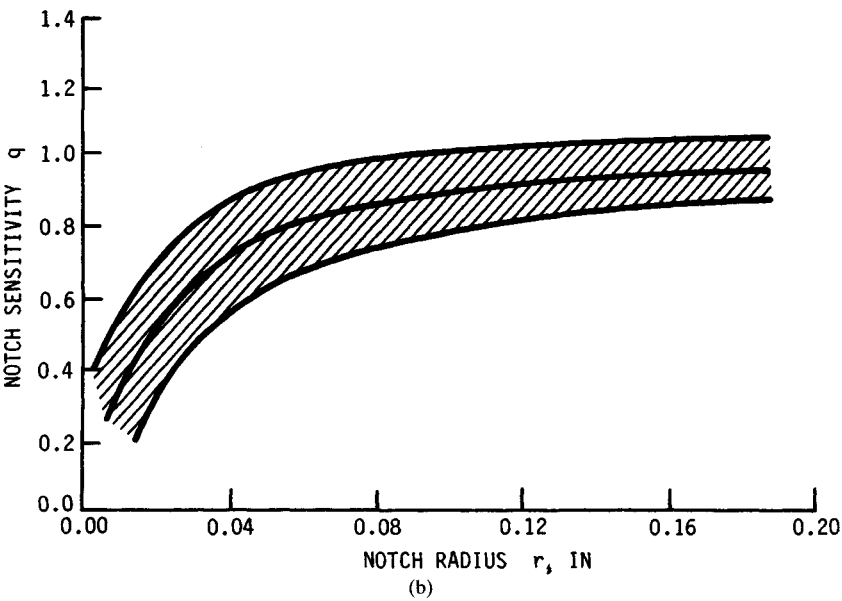

(b)

FIGURE 29.10 Scatter bands of notch sensitivity q as a function of notch radius and heat treatment for undifferentiated steels. (*a*) Quenched and tempered; (*b*) normalized or annealed. *(Adapted from Sines and Waisman [29.16], with permission of McGraw-Hill, Inc.)*

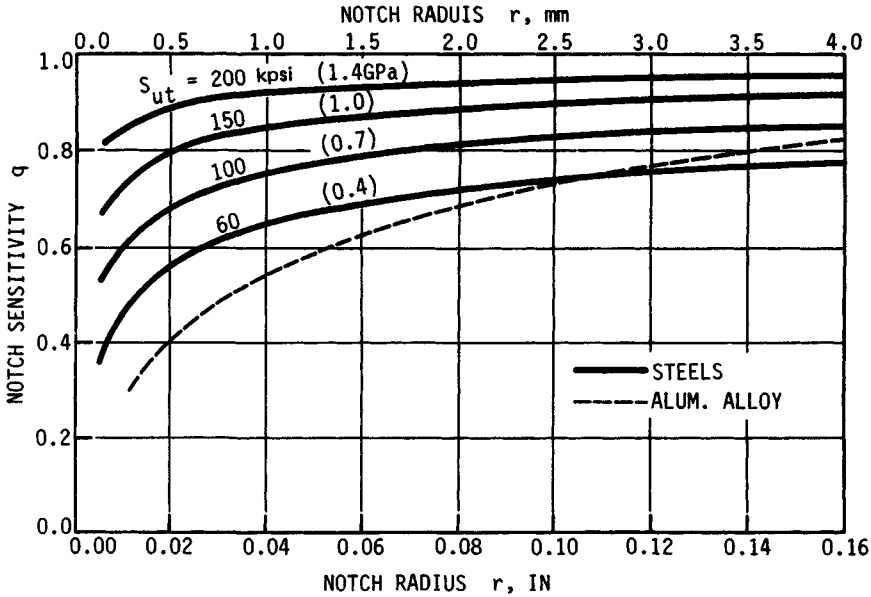

FIGURE 29.11 Notch-sensitivity chart for steels and UNS A92024T wrought aluminum alloys subjected to reversed bending or reversed axial loads. For larger notch radii, use values of q corresponding to $r = 0.16$ in (4 mm). *(From Sines and Waisman [29.16], with permission of McGraw-Hill, Inc.)*

When these effects are present, tests are needed in order to assess the extent of such influences and to form a rational basis for assignment of a fatigue modification factor k_e.

29.4 FLUCTUATING STRESS

Variable loading is often characterized by an amplitude component σ_a as ordinate and a steady component σ_m as abscissa. Defined in terms of maximum stress σ_{max} and minimum stress σ_{min} the coordinates are as follows:

$$\sigma_a = \frac{1}{2}|\sigma_{max} - \sigma_{min}| \qquad \sigma_m = \frac{1}{2}(\sigma_{max} + \sigma_{min}) \tag{29.17}$$

The designer's fatigue diagram is depicted in Fig. 29.12.

If one plots combinations σ_a and σ_m that partition part survival from part failure, a failure locus is defined. Properties such as ultimate tensile strength $\bar{S}_{ut}$, yield strength in tension $\bar{S}_y$, yield strength in compression $\bar{S}_{yc}$, endurance strength $\bar{S}_e$, or fatigue strength $\bar{S}_f$ appear as axis intercepts. In the range in which σ_m is negative and fatigue fracture is a threat, the failure locus is taken as a horizontal line unless specific experimental data allow another locus. In the range in which σ_m is positive, the preferred locus is Gerber or ASME-Elliptic. The Goodman and Soderberg loci have

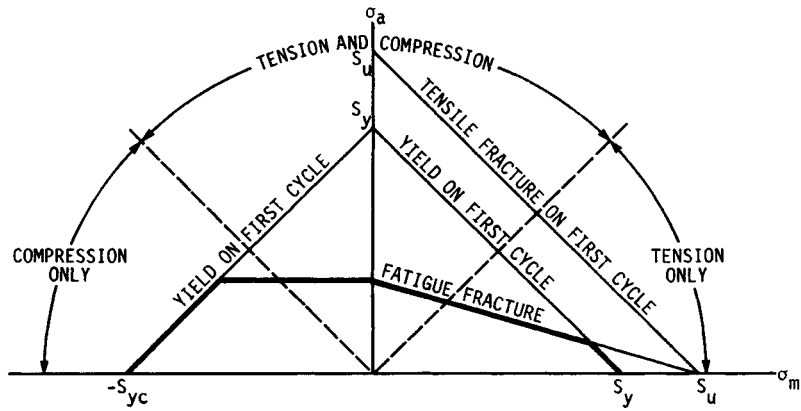

FIGURE 29.12 Designer's fatigue diagram using a Goodman failure locus for push-pull (axial) fatigue.

historical importance and algebraic simplicity, but these loci do not fall centrally among the data, and they are not dependably conservative.

For the Gerber locus,

$$\frac{\sigma_a}{\bar{S}_e} + \left(\frac{\sigma_m}{\bar{S}_{ut}}\right)^2 = 1 \tag{29.18}$$

For the ASME-elliptic fatigue locus,

$$\left(\frac{\sigma_a}{\bar{S}_e}\right)^2 + \left(\frac{\sigma_m}{\bar{S}_y}\right)^2 = 1 \tag{29.19}$$

Brittle materials subject to fluctuating stresses which follow the Smith-Dolan fatigue locus in the first quadrant of the designer's fatigue diagram have

$$\frac{\sigma_a}{\bar{S}_e} = \frac{1 - \sigma_m/\bar{S}_{ut}}{1 + \sigma_m/\bar{S}_{ut}} \tag{29.20}$$

When endurance strengths of steels are plotted against cycles to failure, a logarithmic transformation of each coordinate results in a linear data string in the interval $10^3 \le N \le 10^6$ cycles (see Fig. 29.8). At 10^6 cycles, $\bar{S}_f = \bar{S}_e = \bar{\phi}_{0.30}\bar{S}_{ut}$. At 10^3 cycles, $(\bar{S}_f)_{10^3} = f\bar{S}_{ut}$, where f is a fraction. Arguments in [29.6], p. 279, give

$$f = \frac{S_e}{S_{ut}}\left(\frac{\sigma_f'}{S_e}\right)^{1/2.1} = \frac{S_e}{S_{ut}}\left(\frac{\bar{\sigma}_0\varepsilon_f^m}{S_e}\right)^{1/2.1} \tag{29.21}$$

The fraction of ultimate tensile strength realized at 10^3 cycles is a function of the fatigue ratio $\phi_{0.30}$ and the ultimate tensile strength. The fraction f is in the range $0.8 < f < 1$ for steels. One can estimate f from Eq. (29.21). The constants a and b of $S_f = aN^b$ can then be found from

$$a = \frac{f^2 \bar{S}_{ut}^2}{\bar{S}_e} \tag{29.22}$$

$$b = -\frac{1}{3} \log \frac{f \bar{S}_{ut}}{\bar{S}_e} \tag{29.23}$$

For axial fatigue, the $(\bar{S}_{ax})_{10^3}$ ordinate in Fig. 29.8 is $\bar{k}_c f \bar{S}_{ut}$ and the $(\bar{S}_{ax})_{10^6}$ ordinate is $\bar{k}_c \phi_{0.30} \bar{S}_{ut}$, where $\bar{k}_c$ is determined by interpolation in Table 29.6. For torsional fatigue, the $(\bar{S}_{sf})_{10^3}$ ordinate is $\bar{k}_c f \bar{S}_{ut}$ and the $(\bar{S}_{sf})_{10^6}$ ordinate is $\bar{k}_c \phi_{0.30} \bar{S}_{ut}$, where $\bar{k}_c$ is taken from Table 29.7 or, for materials following the distortion-energy theory of failure closely, $\bar{k}_c = 0.577$.

29.5 COMPLICATED STRESS-VARIATION PATTERNS

Many loading patterns depart from the sinusoidal character of smoothly rotating machinery and the convenient equation pair displayed as Eq. (29.17). In complicated patterns, characterization in the form of maximum force F_{max} (or maximum stress σ_{max}) and minimum force F_{min} (or minimum stress σ_{min}) is more useful. In fact, max-min (max/min/same max or min/max/same min) will avoid losing a damaging cycle.

Consider a full cycle with stresses varying 60, 80, 40, 60 kpsi and another cycle with stresses –40, –60, –20, –40 kpsi, as depicted in Fig. 29.13*a*. These two cycles cannot be imposed on a part by themselves, but in order for this to be a repetitive block, it is necessary to acknowledge the loading shown by the dashed lines. This adds a hidden cycle that is often ignored. To ensure not losing the hidden cycle, begin the analysis block with the largest (or smallest) stress, adding any preceding history to the right end of the analysis block as shown in Fig. 29.13*b*. One now searches for cycles using max-min characterizations. Taking the "hidden" cycle first so that it is not lost, one moves along the trace as shown by the dashed line in Fig. 29.13*b*, identifying a cycle with a maximum of 80 kpsi and a minimum of –60 kpsi. Looking at the

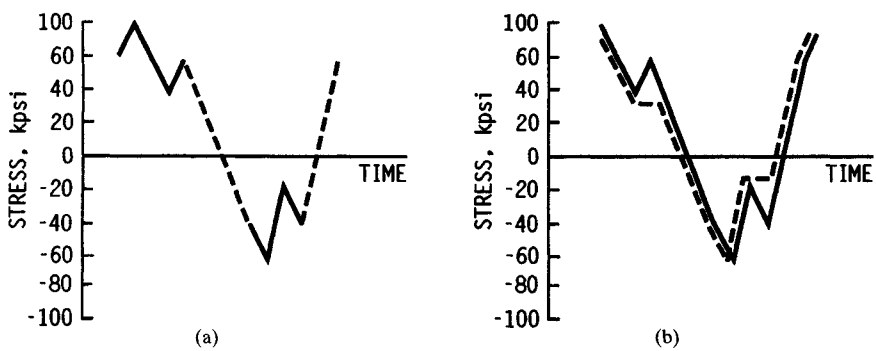

FIGURE 29.13

remaining cycles, one notes a cycle with a maximum of 60 and a minimum of 40 kpsi. There is another with a maximum of –20 and a minimum of –40 kpsi. Since failure theories are expressed in terms of σ_a and σ_m components, one uses Eqs. (29.17) and constructs the table below.

Cycle	σ_{max}	σ_{min}	σ_a	σ_m
1	80	–60	70	10
2	60	40	10	50
3	–20	–40	10	–30

Note that the most damaging cycle, cycle 1, has been identified because care was taken not to lose it. The method used is a variation of the *rainflow counting* technique. One is now ready to apply Miner's rule. Note that if the original cycles were doubled in the block, there would be five cycles, with the additional two duplicating cycles 2 and 3 above.

Example 2. The loading of Fig. 29.13*a* is imposed on a part made of 1045 HR steel. Properties at the critical location are $S_{ut} = 92.5$ kpsi, $S'_e = 46$ kpsi, strain-strengthening coefficient $\bar{\sigma}_0 = 140$ kpsi, true strain at fracture $\varepsilon_f = 0.58$, and strain-strengthening exponent $m = 0.14$. Estimate how many repetitions of the loading block may be applied if a Gerber fatigue locus is used.

Solution. From Eq. (29.21),

$$f = \frac{S_e}{S_{ut}}\left(\frac{\sigma'_f}{S_e}\right)^{1/2.1} = \frac{S_e}{S_{ut}}\left(\frac{\bar{\sigma}_0 \varepsilon_f^m}{S_e}\right)^{1/2.1}$$

$$= \frac{46}{92.5}\left(\frac{140(0.58)^{0.14}}{46}\right)^{1/2.1} = 0.815$$

From Eq. (29.22), $a = \dfrac{0.815^2 92.5^2}{46} = 123.5$ kpsi

From Eq. (29.23),

$$b = -\frac{1}{3}\log\frac{0.815(92.5)}{46} = -0.0715$$

$$(S_f)_{10^3} = fS_{ut} = 0.815(92.5) = 75.39 \text{ kpsi}$$

For cycle 1, which has $\sigma_a = 70$ kpsi and $\sigma_m = 10$ kpsi, using Eq. (29.18),

$$S_f = \frac{\sigma_a}{1 - (\sigma_m/S_{ut})^2} = \frac{70}{1 - (10/92.5)^2} = 70.83 \text{ kpsi}$$

Since required endurance strength 70.83 kpsi is less than $(S_f)_{10^3}$, the number of cycles exceeds 10^3.

$$N_1 = \left(\frac{S_f}{a}\right)^{1/b} = \left(\frac{70.83}{123.5}\right)^{-1/0.0715} = 2383 \text{ cycles}$$

For cycle 2, $S_f = 14.1$ kpsi and $N_2 = 1.5(10^{13}) \doteq \infty$. For cycle 3, $S_f = \sigma_a = 10$ kpsi and $N_3 = 1.8(10^{15}) \doteq \infty$. Extend the previous table:

Cycle	S_f	N
1	70.8	2383
2	14.1	∞
3	10.0	∞

The damage per block application according to Miner's rule is

$$D = \Sigma\,(1/N_i) = 1/2383 + 1/\infty + 1/\infty = 1/2383$$

The number of repetitions of the block is $1/D = 1/(1/2383) = 2383$. For the original two cycles, the damage per block application is $1/\infty + 1/\infty = 0$ and the number of repetitions is infinite. Note the risk of an analysis conclusion associated with not drawing how the cycles connect.

29.6 STRENGTH AT CRITICAL LOCATIONS

The critical locations of strength-limited designs can be identified as regions in which load-induced stresses peak as a result of distribution of bending moment and/or changes in geometry. Since the strength at the critical location in the geometry and at condition of use is required, it is often necessary to reflect the manufacturing process in this estimation. For heat-treatable steels under static loading, an estimate of yield or proof strength is required, and under fatigue loading, an estimate of the ultimate strength of the endurance limit is needed for an adequacy assessment. For the design process, strength as a function of intensity of treatment is required. In Chap. 33, the quantitative estimation methods of Crafts and Lamont and of Grossmann and Field for heat-treatable steels are useful. For cold work and cold heading, the methods of Datsko and Borden give useful estimates.

Consider an eyebolt of cold-formed 1045 steel hot-rolled quarter-inch-diameter rod in the geometry of Fig. 29.14. The properties of the hot-rolled bar are

$$S_y = 60 \text{ kpsi} \qquad m = 0.14 \qquad \bar{\sigma}_o = 140 \text{ kpsi}$$

$$S_u = 92.5 \text{ kpsi} \qquad \varepsilon_f = 0.58$$

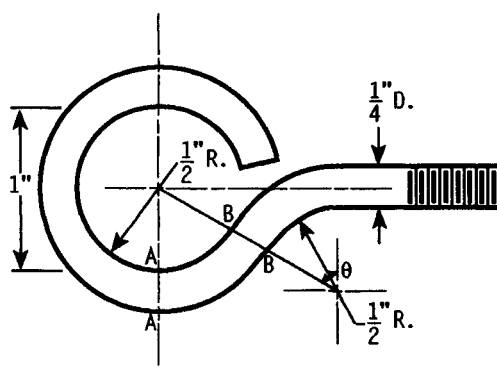

FIGURE 29.14 Geometry of a cold-formed eyebolt.

At section AA on the inside surface, the true strain is estimated as

$$\varepsilon_i = \left|-\frac{1}{2}\ln\left(1+\frac{2d}{D}\right)\right| = \left|-\frac{1}{2}\ln\left[1+\frac{2(0.25)}{1}\right]\right|$$

$$= |-0.203| = 0.203$$

The yield strength of the surface material at this location is estimated as, from Table 33.1,

$$\varepsilon_{quo} = \frac{0.203}{1+1} = 0.1015 \qquad \varepsilon_{qyo} = \frac{0.1015}{1+2(0.1015)} = 0.0844$$

$$(S_y)_{tLc} = \bar{\sigma}_o\,(\varepsilon_{qyo})^m = 140(0.0844)^{0.14} = 99 \text{ kpsi}$$

The ultimate strength at this location is estimated as, from Table 33.1,

$$(S_u)_{tLc} = (S_u)_o \exp(\varepsilon_{quo}) = 92.5 \exp(0.1015) = 102.4 \text{ kpsi}$$

Both the yield strength and the ultimate strength have increased. They are nominally equal because the true strain of 0.203 exceeds the true strain of 0.14 which occurs at ultimate load. The yield strength has increased by 65 percent and the ultimate strength has increased by 11 percent at this location. The strength at the inside and outside surface at section BB has not changed appreciably. The changes at the sections above BB are improvements in accord with the local geometry. For dynamic strength, the endurance limits have changed in proportion to the changes in ultimate strength. At section AA the R. R. Moore endurance limit is estimated to be

$$S'_e = \frac{S_u}{2} = \frac{102.4}{2} = 51.2 \text{ kpsi}$$

an improvement of 11 percent. Since the strengths vary with position and stresses vary with position also, a check is in order to see if section AA or section BB is critical in a tensile loading of the eyebolt.

The increase in yield strength and endurance limit due to cold work, while present, may not be helpful. Consider the strip spring formed from bar stock to the geometry of Fig. 29.15. Just to the right of the radius the original properties prevail, and the bending moment is only slightly less than to the left of section AA. In this case, the increased strength at the critical location is not really exploitable.

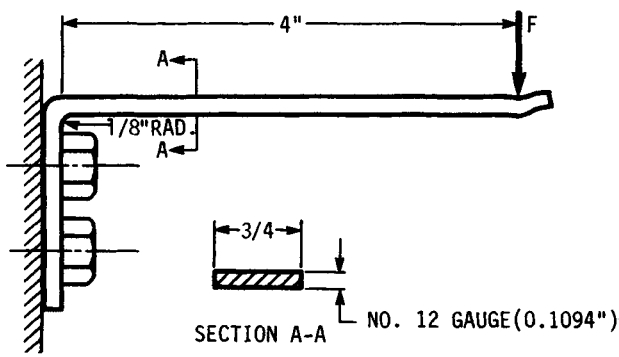

FIGURE 29.15 A latching spring cold formed from ¾-in-wide No. 12 gauge strip.

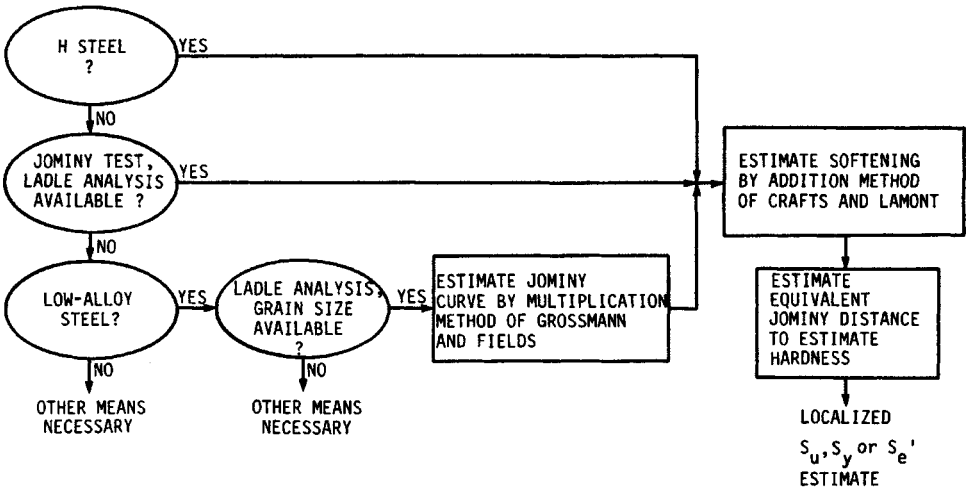

FIGURE 29.16 Logic flowchart for estimation of localized ultimate strength or endurance limit for heat-treated steels.

For parts that are heat-treated by quenching and tempering, the methods and procedures are given in Fig. 29.16 (see Chap. 33). If a shaft has been designed, an adequacy assessment is required. An estimate of the strength at a location where the shaft steps in Fig. 29.17 from 1 to 1.125 in is necessary. The specifications include the material to be 4140 steel quenched in still oil with mild part agitation and tempered for 2 hours at 1000°F. The material earmarked for manufacture has a ladle analysis of

	C	Mn	P	S	Si	Ni	Cr	Mo
Percent	0.40	0.83	0.012	0.009	0.26	0.11	0.94	0.21
Multiplier	0.207	3.87	—	—	1.18	1.04	3.04	1.65

The experience is that a grain size of 7½ can be maintained with this material and heat treatment. The multipliers are determined by the methods of Chap. 33. The ideal critical diameter is estimated as

$$D_I = 0.207(3.87)(1.18)(1.04)(3.04)(1.65) = 4.93 \text{ in}$$

The factors are $D = 5.3$, $B = 10$, and $f = 0.34$. The addition factors are

$$A_{Mn} = 2.1$$

$$A_{Si} = 1.1$$

$$A_{Ni} = 0.03$$

$$A_{Cr} = 4.9$$

$$A_{Mo} = 3.78$$

$$\Sigma A = 11.91$$

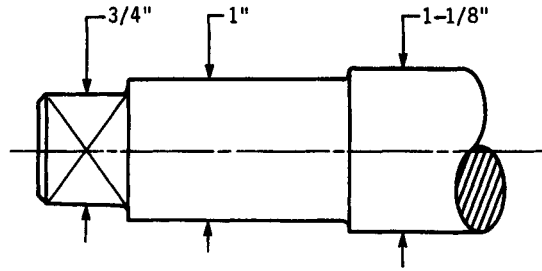

FIGURE 29.17 A portion of a 4140 steel shaft quenched in still oil ($H = 0.35$) and tempered for 2 hours at 1000°F, grain size 7.5.

The tempered hardness equation becomes

$$R_T = (R_Q - 5.3 - 10)0.34 + 10 + 11.91 = 0.34R_Q + 16.71$$

The Jominy curve is predicted by noting that the Rockwell C-scale hardness at Jominy station 1 is

$$(R_Q)_1 = 32 + 60(\%C) = 32 + 60(0.40) = 56.0$$

and a table is prepared as depicted in Table 29.9 for 1000°F tempering temperature. The variation of surface strength with size of round is prepared using equivalent Jominy distances as depicted in Table 29.10. Table 29.11 shows an ultimate-strength traverse of a 1⅛-in round. There is only a mild strength profile in the traverse. The significant strength for bending and torsion is at the surface. For the 1⅛-in round, the surface ultimate strength is estimated by interpolation to be 164.3 kpsi. The R. R. Moore endurance limit at this location is estimated to be 164.3/2, or 82 kpsi. Steels in large sections or with less alloying ingredients (smaller ideal critical diameters) exhibit larger transverse strength changes. For sections in tension, significant strength is at the center. When testing, machined specimens from the center of a round say little about the strength at the surface. Heat treating a specimen proves little about strengths in the actual part. Some variations in strength attributed to size result from differences in cooling rates.

When the number of cycles is less than 10^7, the endurance strength must be estimated. Reference [29.8] gives a useful curve fit for steels:

$$S'_f = \begin{cases} S_u m^{-m} \exp(m) \varepsilon_f^m N_f^{cm} \exp(-\varepsilon_f N_f^c) & \varepsilon_f N_f^c \le m \\ S_u & \varepsilon_f N_f^c > m \end{cases} \tag{29.24}$$

TABLE 29.9 Surface Ultimate Strength as a Function of Jominy Distance for 4140 Steel Oil Quenched ($H = 0.35$) and Tempered 2 Hours at 1000°F, Grain Size 7½

Jominy distance, $\frac{1}{16}$ in	IH/DH	Predicted Jominy R_Q, Rockwell C	Tempered hardness R_T, Rockwell C	Surface ultimate strength S_u, kpsi
1	1	56.0	44.1	206.6
4	1	56.0	44.1	206.6
8	1.09	51.4	42.0	196.0
12	1.18	47.5	40.3	187.5

TABLE 29.10 Variation of Surface Strength with Diameter of 4140 Steel Round Quenched in Still Oil ($H = 0.35$) and Tempered for 2 Hours at 1000°F, Grain Size 7½

Diameter, in	Equivalent Jominy distance, $\frac{1}{16}$ in	Surface ultimate strength, kpsi
0.1	1.0	167
0.5	2.7	167
1	5.1	165
2	8.2	159.1
3	10.0	156.1
4	11.4	153.2

where m = strain-strengthening exponent
ε_f = true strain at fracture
c = an exponent commonly in the neighborhood of $-\frac{1}{2}$
N_f = the number of cycles to failure
S_u = ultimate tensile strength

Example 3. Estimate the finite-life engineering fatigue strength of an annealed 4340 steel with the following properties:

$$S_u = 103 \text{ kpsi} \qquad S_y = 65.6 \text{ kpsi at 0.2 percent offset}$$

$$RA = 0.56$$

Solution. The endurance limit is estimated as $S_u/2 = 103/2 = 51.5$ kpsi at 10^7 cycles. Because no strain-hardening information is supplied, it is necessary to estimate m from

$$\frac{S_u}{S_y} = \left[\frac{m}{(\text{offset}) \exp 1}\right]^m$$

or

$$\frac{103}{65.6} - \left[\frac{m}{0.002(2.718)}\right]^m = 0$$

from which $m = 0.14$. The true strain at fracture can be assessed from the reduction in area:

$$\varepsilon_f = \ln \frac{1}{1 - RA} = \ln \frac{1}{1 - 0.56} = 0.821$$

TABLE 29.11 Variation of Local Strength in a 1.125-in Round of 4140 Steel Quenched in Still Oil ($H = 0.35$) and Tempered for 2 Hours at 1000°F, Grain Size 7½

Radial position	Equivalent Jominy distance, $\frac{1}{16}$ in	Local ultimate strength, kpsi
(0)r	7.33	161.0
0.5r	6.35	162.8
0.8r	5.95	163.5
r	5.55	164.2

The true stress coefficient of the strain-strengthening equation $\bar{\sigma} = \bar{\sigma}_o \varepsilon^m$ is

$$\bar{\sigma}_o = S_u m^{-m} \exp m = 103(0.14)^{-0.14} \exp 0.14$$

$$= 156.0 \text{ kpsi}$$

The constructive strain ε_1 is a root of the equation

$$\frac{\bar{\sigma}_o}{S'_e} \varepsilon_1^m \exp(-\varepsilon_1) - 1 = 0$$

or alternatively,

$$\frac{S_u}{S'_e} m^{-m} \exp(m) \varepsilon_1^m \exp(-\varepsilon_1) - 1 = 0$$

When ε_1 is small, the term $\exp -\varepsilon_1$ approaches 1, and ε_1 can be found explicitly from

$$\varepsilon_1 = \left(\frac{S'_e}{\bar{\sigma}_o}\right)^{1/m} \quad \text{or} \quad \varepsilon_1 = \frac{m}{2.718}\left(\frac{S'_e}{S_u}\right)^{1/m}$$

From the first,

$$\varepsilon_1 = \left(\frac{51.5}{156}\right)^{1/0.14} = 0.000365$$

This value of the constructive strain allows estimation of the exponent c from $\varepsilon_1 = \varepsilon_f N_f^c$:

$$c = \frac{\log \varepsilon_1/\varepsilon_f}{\log N_e} = \frac{\log(0.000\,365/0.821)}{\log 10^7} = -0.4788$$

Now Eq. (29.24) can be written as

$$S'_f = 103(0.14)^{-0.14} \exp(0.14) 0.821^{0.14} N_f^{-0.4778(0.14)} \exp(0.821 N_f^{-0.4788})$$

which simplifies to

$$S'_f = 151.8 N_f^{-0.067} \exp(0.821 N_f^{-0.4788})$$

Table 29.12 can be constructed. See Ref. [29.8] for notch-sensitivity corrections for low cycle strengths.

29.7 COMBINED LOADING

Simple loading is regarded as an influence that results in tension, compression, shear, bending, or torsion, and the stress fields that result are regarded as simple. *Combined loading* is the application of two or more of these simple loading schemes. The stresses that result from both simple and combined loading are three-dimensional. Applying the adjective *combined* to stresses is inappropriate. The nature of both yielding and fatigue for ductile materials is best explained by distortion-energy (octahedral shear, Henckey-von Mises) theory. For variable loading, the stress state is plotted on a modified Goodman diagram that has tensile mean stresses as abscissa and

TABLE 29.12 Fatigue Strength Ratio S_f'/S_u as a Function of Cycles to Failure for Annealed 4340 Steel†

Number of cycles-to-failure N_f	Constructive true strain ε_1	Endurance strength S_f, kpsi	Ratio S_f'/S_u
10^0	0.821	103‡	1‡
10^1	0.273	103‡	1‡
10^2	0.091	101.8	0.99
10^3	0.030	92.7	0.90
10^4	0.010	81.0	0.79
10^5	0.0033	69.9	0.68
10^6	0.0011	60.1	0.58
10^7	0.000 37	51.5	0.50

†S_u = 103 kpsi, S_y = 65.6 kpsi (0.002 offset), reduction in area 56 percent.
‡Since $\varepsilon_1 > m$, $S_f' = S_u$ and $S_f'/S_u = 1$.

tensile stress amplitude as ordinate. The stress amplitude is that present in a uniform tension that induces the same distortion-energy amplitude (octahedral shear amplitude) as is present in the critical location of the machine part. The steady stress is that stress present in a uniform tension that induces the same steady distortion energy (steady octahedral shear) as is present in the critical location of the machine part. The plotting process involves conversion of the actual stress state to the equivalent uniform tension circumstances.

The von Mises axial tensile stress that has the same distortion energy as a general three-dimensional stress field is, in terms of the ordered principal stresses σ_1, σ_2, and σ_3,

$$\sigma_v = \left[\frac{(\sigma_1 - \sigma_2)^2 + (\sigma_2 - \sigma_3)^2 + (\sigma_3 - \sigma_1)^2}{2}\right]^{1/2} \tag{29.25}$$

If one of the principal stresses is zero and the other two are σ_A and σ_B, then

$$\sigma_v = (\sigma_A^2 + \sigma_B^2 - \sigma_A\sigma_B)^{1/2} \tag{29.26}$$

If the axes xy are not principal, then

$$\sigma_v = (\sigma_x^2 + \sigma_y^2 - \sigma_x\sigma_y + 3\tau_{xy}^2)^{1/2} \tag{29.27}$$

If the concern is yielding, then yielding begins when the von Mises stress equals the tensile value of S_y. If the concern is fatigue, then failure occurs when the von Mises steady stress and amplitude equal the simple steady tension and amplitude that result in failure. If Eq. (29.26) is equated to a critical value σ_{cr}, then

$$\sigma_A^2 + \sigma_B^2 - \sigma_A\sigma_B = \sigma_{cr}^2$$

Treating the preceding equation as a quadratic in σ_A, we have

$$\sigma_A = \frac{1}{2}\sigma_B \pm \frac{1}{2}\sqrt{(2\sigma_{cr})^2 - 3\sigma_B^2} \tag{29.28}$$

On a plot in the $\sigma_A\sigma_B$ plane, the critical-stress magnitude can be observed at six places, three tensile and three compressive. The locus is an ellipse with the major axis

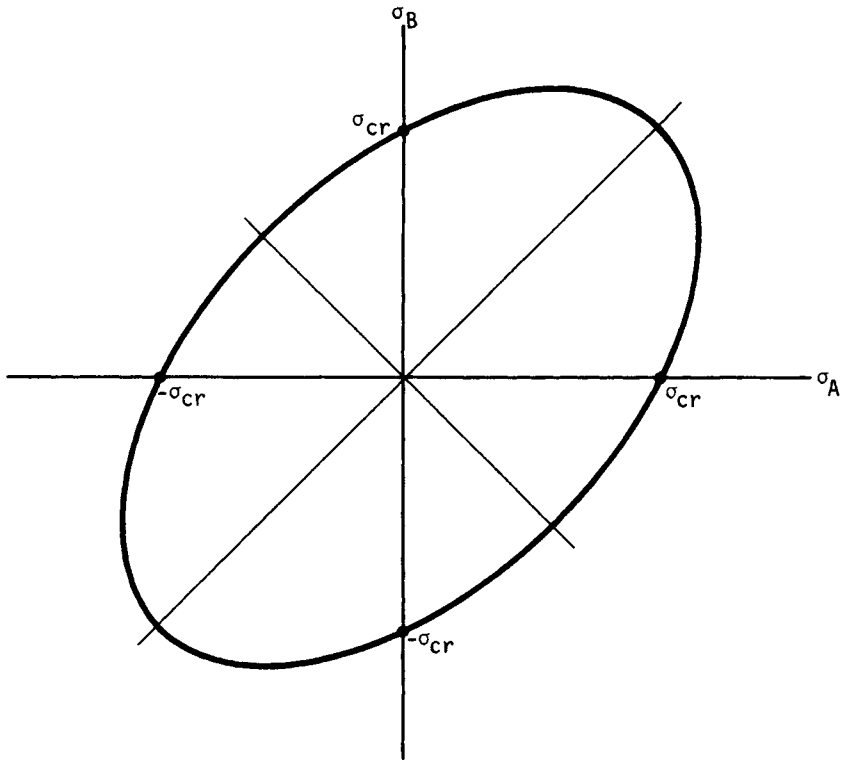

FIGURE 29.18 The distortion-energy critical-stress ellipse. For any point σ_A, σ_B on the ellipse, the uniaxial tension with the same distortion energy is the positive abscissa intercept σ_{cr}, 0.

having a unity slope, as depicted in Fig. 29.18. The octahedral stress (von Mises stress) tensile equivalent is the σ_A-axis intercept of the ellipse. For the Goodman diagram, the transformation is to move the point representing the stress condition σ_A, σ_B to the abscissa, while staying on the ellipse. This is done by Eq. (29.26). For three-dimensional stress, the surface is an ellipsoid in the $\sigma_1\sigma_2\sigma_3$ space, and the transformation is accomplished by Eq. (29.25). Figure 29.19 shows the conversions of the steady-stress condition and the stress-amplitude condition to the respective simple-tension equivalents for the purposes of plotting a point representing the equivalent stress state on the modified Goodman diagram. In Fig. 29.20 an element on a shaft sees a steady torque and fully reversed bending stresses. For the steady-stress element,

$$\tau_{xym} = \frac{16T}{\pi d^3} \qquad \sigma_{Am} = \frac{16T}{\pi d^3} \qquad \sigma_{Bm} = -\frac{16T}{\pi d^3}$$

and the corresponding von Mises stress is

$$\sigma_{vm} = (\sigma_{Am}^2 + \sigma_{Bm}^2 - \sigma_{Am}\sigma_{Bm})^{1/2} = \frac{\sqrt{3}\,16T}{\pi d^3}$$

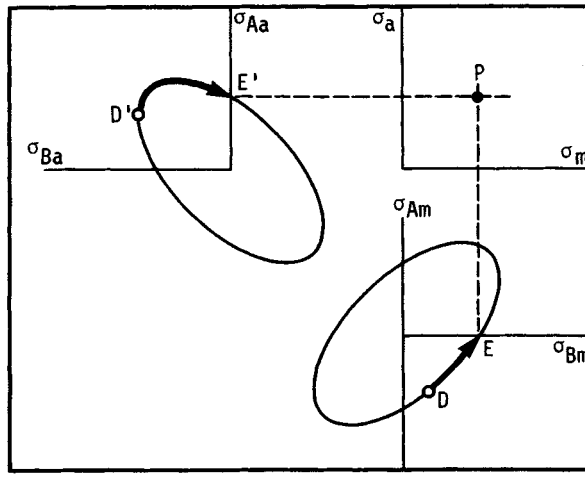

FIGURE 29.19 The principal stresses due to the steady stresses σ_{Am} and σ_{Bm} appear on the distortion-energy ellipse as point *D*. The transform to equivalent distortion energy in tension is point *E*, which becomes the abscissa of point *P*. The principal stresses due to stress amplitude σ_{Aa} and σ_{Ba} appear as point *D'*; the transform is *E'*, which becomes the ordinate of point *P*.

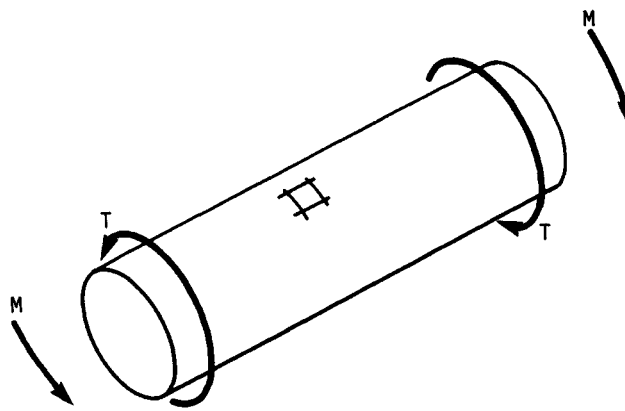

(a)

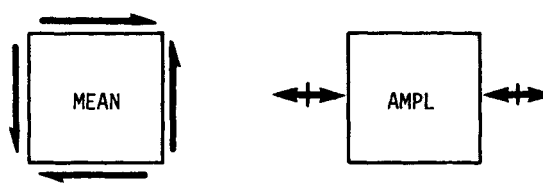

(b)

FIGURE 29.20 (*a*) A shaft subjected to a steady torque *T* and completely reversed flexure due to bending moment *M*; (*b*) the mean-stress element and the stress-amplitude element.

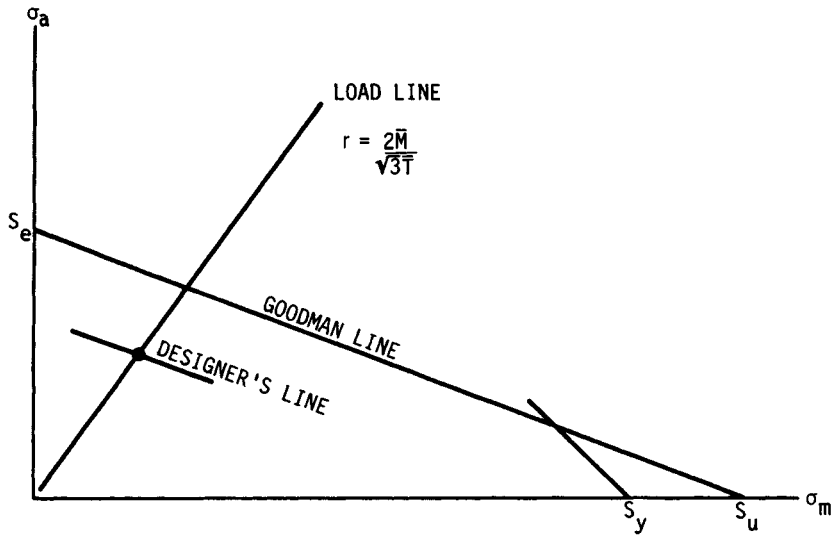

FIGURE 29.21 Designer's fatigue diagram for geared shaft showing load line of slope $r = 2M/(\sqrt{3}T)$, the operating point P, using the Goodman failure locus, and the designer's line reflecting a design factor of n.

For the amplitude-stress element,

$$\sigma_{x,\max} = \frac{32M}{\pi d^3} \qquad \sigma_{x,\min} = -\frac{32M}{\pi d^3}$$

$$\sigma_{Aa} = \frac{32M}{\pi d^3} \qquad \sigma_{Ba} = 0$$

and the corresponding von Mises stress is

$$\sigma_{va} = (\sigma_{Aa}^2 + \sigma_{Ba}^2 - \sigma_{Aa}\sigma_{Ba})^{1/2} = \frac{32M}{\pi d^3}$$

If this is an element of a geared shaft, then M and T are proportional and the locus of possible points is a radial line from the origin with a slope of

$$r = \frac{\sigma_{va}}{\sigma_{vm}} = \frac{32M}{\pi d^3} \frac{\pi d^3}{\sqrt{3}\,16T} = \frac{2M}{\sqrt{3}T} \tag{29.29}$$

This is called the *load line.* If data on failures have been collected and converted to von Mises components and a Goodman line is an adequate representation of the failure locus, then for the designer's line in Fig. 29.21,

$$\frac{\sigma_{va}}{S_e} + \frac{\sigma_{vm}}{S_u} = \frac{1}{n} \tag{29.30}$$

where n = design factor. Substituting for σ_{va} and σ_{vm} and solving for d, we obtain

$$d = \left[\frac{32n}{\pi}\left(\frac{M}{S_e} + \frac{\sqrt{3}T}{2S_u}\right)\right]^{1/3} \tag{29.31}$$

Data points representing failure are plotted embracing a significant stress commitment, and the plotted load line represents the same belief. It is appropriate that equations such as Eq. (29.31) be labeled with two adjectives: (1) *significant stress* and (2) *failure locus.* For example, Eq. (29.31) could be called a distortion-energy Goodman equation.

For the case where moments, torques, and thrusts contribute both steady and alternating components of stress, then the distortion-energy Goodman equation for the critical location is

$$\frac{16}{\pi d^3 S_e}\left[\left(2M_a + \frac{P_a d}{4}\right)^2 + 3T_a^2\right]^{1/2} + \frac{16}{\pi d^3 S_u}\left[\left(2M_m + \frac{P_m d}{4}\right)^2 + 3T_m^2\right]^{1/2} - \frac{1}{n} = 0 \quad (29.32)$$

where n = design factor
M_a = component of bending moment causing flexural stress amplitude
M_m = component of bending moment causing flexural stress, steady
T_a = component of torque causing shear-stress amplitude
T_m = component of torque causing shear stress, steady
P_a = component of axial thrust causing tensile-stress amplitude
P_m = component of axial thrust causing tensile stress, steady
S_e = local fatigue strength of shaft material
S_u = ultimate local tensile strength
d = local shaft diameter

Since the equation cannot be solved for d explicitly, numerical methods are used.

29.8 SURFACE FATIGUE

When cylinders are in line contact, sustained by a force F, a flattened rectangular zone exists in which the pressure distribution is elliptical. The half width of the contact zone b is

$$b = \sqrt{\frac{2F}{\pi\ell}\frac{[1-\nu_1^2]/E_1 + [1-\nu_2^2]/E_2}{(1/d_1) + (1/d_2)}} \quad (29.33)$$

The largest stress in magnitude is compressive and exists on the z axis. As a pressure, its magnitude is

$$p_{\max} = \frac{2F}{\pi b \ell} \quad (29.34)$$

Along the z axis, the orthogonal stresses are [29.6]

$$\sigma_x = -2p_{\max}\left[\sqrt{1 + \left(\frac{z}{b}\right)^2} - \frac{z}{b}\right] \quad (29.35)$$

$$\sigma_y = -p_{\max}\left\{\left[2 - \frac{1}{1 + (z/b)^2}\right]\sqrt{1 + \left(\frac{z}{b}\right)^2} - 2\frac{z}{b}\right\} \quad (29.36)$$

$$\sigma_z = \frac{-p_{\max}}{\sqrt{1 + (z/b)^2}} \quad (29.37)$$

These equations can be useful with rolling contact, such as occurs in cams, roller bearings, and gear teeth. The approach of the center of the rollers is

$$\Delta = \frac{2F}{\pi \ell}\left(\frac{1-\nu_1^2}{E_1} + \frac{1-\nu_2^2}{E_2}\right)\left(\ln\frac{d_1}{b} + \ln\frac{d_2}{b} + \frac{2}{3}\right) \tag{29.38}$$

The largest principal stress is compressive and located at the center of the rectangular flat and is $-p_{\max}$ in magnitude. The largest shear stress is approximately $0.30p_{\max}$ and is located at about $0.78b$ below the surface. The maximum compressive stress is repeatedly applied in rolling cylinders. At a position of $z = 0.4b$, $y = 0.915b$ the shear stress has a magnitude of $0.242p_{\max}$ but is completely reversed in rolling cylinders.

The loss of surface integrity due to repeated application of hertzian contact stresses is called *surface fatigue.* The phenomenon is marked by the loss of material from the surface, leaving pits or voids. The onset of fatigue is often defined as the appearance of craters larger than a specified breadth. If Eq. (29.33) is substituted into Eq. (29.34) and the magnitude of $p_{\max}$ associated with the first tangible evidence of fatigue at a specified number of cycles is called the *surface endurance strength* S_{fe}, then

$$\frac{F}{\ell}\left(\frac{2}{d_1} + \frac{2}{d_2}\right) = \pi S_{fe}^2\left(\frac{1-\nu_1^2}{E_1} + \frac{1-\nu_2^2}{E_2}\right) = K \tag{29.39}$$

The left-hand side of the equation consists of parameters under the designer's control. The right-hand side consists of materials properties. The factor K is called *Buckingham's load-stress factor* and is associated with a number of cycles. In gear studies a similar K factor is used and is related to K through

$$K_g = \frac{K}{4}\sin\phi \tag{29.40}$$

where ϕ = gear-tooth pressure angle. Note that $p_{\max}$ is proportional to other stresses present, and it is conventional to describe surface fatigue in terms of the strength S_{fe}. Reference [29.1] gives K_g information for pressure angles of $\phi = 14\frac{1}{2}$ degrees and $\phi = 20$ degrees, as well as S_{fe} for various materials and numbers of cycles. The implication in the literature that above various cycles K_g does not change is unsupported. Log-log plots of K or K_g versus cycles to failure produce "parallel" lines with some consistency in slope for classes of material. AGMA standard 218.01 (Dec. 1982) suggests allowable contact-stress numbers for steel as high as

$$(\sigma)_{10^7} = 0.364H_B + 27 \text{ kpsi} \tag{29.41}$$

for 10^7 cycles, and for the curve fit for other than 10^7 cycles,

$$\sigma_N = C_L\sigma_{10^7} = 2.46N^{-0.056}(0.364H_B + 27) \text{ kpsi} \tag{29.42}$$

For applications where little or no pitting is permissible, the slope of –0.056 persists to 10^{10} (end of presentation). Another curve fit to S_{fe} data for steel at 10^8 cycles is

$$(S_{fe})_{10^8} = 0.4H_B - 10 \text{ kpsi} \tag{29.43}$$

When a gear and pinion are in mesh, the number of cycles to which a point on the tooth surface is exposed is different. Consequently, the material strengths can be tuned to have both pinion and gear show tangible signs of wear simultaneously. For steel gears, using Eq. (29.43), the appropriate gear hardness BHN for a stipulated pinion hardness bhn is

$$\text{BHN} = m_G^{b/2}(\text{bhn} - 25) + 25 \tag{29.44}$$

where m_G = gear ratio, i.e., teeth on the gear per tooth on the pinion. This matching can be done by controlling surface hardness. Strength matching for bending resistance is accomplished by control of core properties.

When needle bearings are specified, the needle assembly is a vendor's product, but the roller track is supplied by the user and is a design concern. The equivalent load F_{eq} accumulating the same damage as a variable radial load F is

$$F_{eq} = \left(\frac{1}{2\pi} \int_0^{2\pi} F^a \, d\theta \right)^{1/a}$$

If the entire assembly is vendor-supplied as a needle-bearing cam follower, then the average load is dictated by the cam-follower force F_{23}. The follower makes m turns per cam revolution. The follower's first turn has an average load to the a power of

$$(F_{23})_1^a = \frac{1}{2\pi/m} \int_0^{2\pi/m} F_{23}^a \, d\theta$$

where $d\theta$ = cam angular displacement. The subsequent averages are

$$(F_{23})_2^a = \frac{1}{2\pi/m} \int_{2\pi/m}^{4\pi/m} F_{23}^a \, d\theta$$

$$\vdots$$

The global average to the a power is

$$F_{\text{global}}^a = \frac{1}{m} \sum_{i=1}^{m} (F_{23})_i^a = \frac{1}{2\pi} \int_0^{2\pi} F_{23}^a \, d\theta$$

Consequently, the roller average radial load is identical to the cam's, but the follower makes m times as many turns.

The follower contact surface between the cam and follower has an endurance strength cycles-to-failure relation of the form of $S^{-1/b}N = K$, and so the average hertzian stress can be written

$$\begin{aligned} \bar{\sigma}_H &= \left(\frac{1}{2\pi} \int_0^{2\pi} \sigma_H^{-1/b} \, d\theta \right)^{-b} \\ &= \frac{C_p}{\sqrt{w}} \left\{ \frac{1}{2\pi} \int_0^{2\pi} [F_{23}(K_c + K_r)]^{-1/2b} \, d\theta \right\}^{-b} \end{aligned} \tag{29.45}$$

where θ = cam rotation angle, b = slope of the rectified SN locus, w = width of the roller or cam (whichever is less), C_p = a joint materials constant

$$C_p = \sqrt{\frac{1}{\pi \left(\dfrac{1-\nu_1^2}{E_1} + \dfrac{1-\nu_2^2}{E_2} \right)}} \tag{29.46}$$

and the parameters K_c and K_r = the curvatures of the cam and roller surfaces, respectively.

One surface location on the cam sees the most intense hertzian stress every revolution. That spot has a hertzian stress of

$$\sigma_H = \frac{C_p}{\sqrt{w}} [F_{23}(K_c + K_r)]_{\max}^{1/2} \tag{29.47}$$

Relative strengths can be assessed by noting that the cam requires a strength of $(S_{fe})_{mN}$ at the critical location in order to survive N cycles. The roller sees the average stress everywhere on its periphery mN times, and its strength requirement is $(S_{fe})_{mN}$. The strength ratio is

$$\frac{[(S_{fe})_N]_{\text{cam}}}{[(S_{fe})_{mN}]_{\text{roller}}} = \frac{[F_{23}(K_c + K_r)]_{\max}^{1/2}}{\left\{\frac{1}{2\pi}\int_0^{2\pi} [F_{23}(K_c + K_r)]^{-1/2b}\, d\theta\right\}^{-b}} = \frac{\sqrt{\mathcal{F}_{\max}}}{(\sqrt{\mathcal{F}})_{\text{avg}}}$$

If cam and roller are steel,

$$(S_{fe})_{mN} = m^b (S_{fe})_N$$

enabling us to place endurance strengths on the same life basis, namely, N, which is convenient when consulting tables of Buckingham load-strength data giving K or its equivalent. Thus,

$$\frac{[(S_{fe})_N]_{\text{cam}}}{[(S_{fe})_N]_{\text{roller}}} = \frac{m^b \sqrt{\mathcal{F}_{\max}}}{(\sqrt{\mathcal{F}})_{\text{avg}}}$$

For steel, a 10^8 cycle expression, that is, $(S_{fe}) = 0.4H_B - 10$ kpsi, can be used. Using bhn for roller Brinell hardness and BHN for cam Brinell hardness, we can write

$$\text{BHN} = \frac{m^b \sqrt{\mathcal{F}_{\max}}}{(\sqrt{\mathcal{F}})_{\text{avg}}} (\text{bhn} - 25) + 25 \tag{29.48}$$

This form is convenient because the roller follower is often a vendor-supplied item and the cam is manufactured elsewhere. Since $\sqrt{\mathcal{F}_{\max}}$ is larger than $(\sqrt{\mathcal{F}})_{\text{avg}}$, this alone tends to require that the cam be harder, but since the roller endures more turns, the roller should be harder, since $m > 1$ and $b < 0$. Matching (tuning) the respective hardnesses so that the cam and roller will wear out together is often a design goal.

Design factor can be introduced by reducing strength rather than increasing load (not equivalent when stress is not directly proportional to load). Since the loads are often more accurately known than strengths in these applications, design factors are applied to strength. The relative hardnesses are unaffected by design factor, but the necessary widths are

$$w = \left(\frac{C_p}{S_{fe}/n}\right)^2_{\text{cam}} \mathcal{F}_{\max} \qquad w = \left(\frac{C_p}{S_{fe}/n}\right)^2_{\text{roller}} (\sqrt{\mathcal{F}})_{\text{avg}} m^{-2b} \tag{29.49}$$

Either equation may be used. The width decision controls the median cycles to failure.

REFERENCES

29.1 R. C. Juvinall, *Stress Strain and Strength,* McGraw-Hill, New York, 1967, p. 218.

29.2 E. M. Prot, "Fatigue Testing under Progressive Loading: A New Technique for Testing Materials," E. J. Ward (trans.), Wright Air Development Center Tech. Rep., TR52-148, September 1952.

29.3 J. A. Collins, *Failure of Materials in Mechanical Design,* Wiley-Interscience, New York, 1981, chap. 10.

29.4 W. J. Dixon and F. J. Massey, Jr., *Introduction to Statistical Analysis,* 3d ed., McGraw-Hill, New York, 1969, p. 380.

29.5 J. T. Ransom, *Statistical Aspects of Fatigue,* Special Technical Publication No. 121, American Society for Testing Materials, Philadelphia, Pa., 1952, p. 61.

29.6 J. E. Shigley and C. R. Mischke, *Mechanical Engineering Design,* 5th ed., McGraw-Hill, New York, 1989.

29.7 C. R. Mischke, "A Probabilistic Model of Size Effect in Fatigue Strength of Rounds in Bending and Torsion," *Transactions of ASME, Journal of Machine Design,* vol. 102, no. 1, January 1980, pp. 32–37.

29.8 C. R. Mischke, "A Rationale for Mechanical Design to a Reliability Specification," *Proceedings of the Design Engineering Technical Conference of ASME,* American Society of Mechanical Engineers, New York, 1974, pp. 221–248.

29.9 L. Sors, *Fatigue Design of Machine Components,* Part 1, Pergamon Press, Oxford, 1971, pp. 9–13.

29.10 H. J. Grover, S. A. Gordon, and L. R. Jackson, *Fatigue of Metals and Structures,* Bureau of Naval Weapons Document NAVWEPS 00-25-534, Washington, D.C., 1960, pp. 282–314.

29.11 C. Lipson and R. C. Juvinall, *Handbook of Stress and Strength,* Macmillan, New York, 1963.

29.12 R. C. Juvinall, *Fundamentals of Machine Component Design,* John Wiley & Sons, New York, 1983.

29.13 A. D. Deutschman, W. J. Michels, and C. E. Wilson, *Machine Design,* MacMillan, New York, 1975.

29.14 E. B. Haugen, *Probabilistic Mechanical Design,* John Wiley & Sons, New York, 1980.

29.15 C. R. Mischke, *Mathematical Model Building,* 2d rev. ed., Iowa State University Press, Ames, 1980.

29.16 G. Sines and J. L. Waisman (eds.), *Metal Fatigue,* McGraw-Hill, New York, 1959.

29.17 H. O. Fuchs and R. I. Stephens, *Metal Fatigue in Engineering,* John Wiley & Sons, New York, 1980.

RECOMMENDED READING

Proceedings of the Society of Automotive Engineers Fatigue Conference, P109, Warrendale, Pa. April 1982.